RESEARCH

Projected changes in rainfall and temperature using CMIP6 models over the Okavango River basin, southern Africa

O. Moses[1]

Abstract

The Okavango River Basin (ORB) which includes a renowned World Heritage site Okavango Delta, contains highly bio-diverse ecosystems. Most of its rural population relies on rain-fed subsistence farming. Limited research has been done on future changes in rainfall and temperature in this region. Here, such changes are analysed for the periods 2030–2059 (near term) and 2070–2099 (long term), relative to the historical period 1985–2014. The analysis is based on the Coupled Model Intercomparison Project Phase 6 (CMIP6), under the shared socioeconomic pathways (SSPs) SSP245 and SSP585. The projected changes vary over the ORB. For rainfall, the models project some significant decreasing trends over Ngamiland in the central/southern ORB, but none are significant over the northern ORB. The significant trends during the near term period include those projected by the model average (-30.60 mm/decade) in March–April (MA) under the SSP585 scenario. Some significant decreasing rainfall trends have also been found in December-February (DJF), but none are significant in October–November (ON). DJF is the main growing season whereas ON (MA) is the onset (end) of the rainy season. For temperature, significant warming trends have been found over both Ngamiland and the northern ORB, with the strongest warming in ON particularly during the near term period. For this ON season over the northern ORB, under the SSP585 (SSP245) scenario, the model average projects a warming trend of 0.56 °C/decade (0.67 °C/decade). These findings may help with the management of agricultural activities, water resources and the highly biodiverse ecosystems in the ORB.

1 Introduction

Climate change has significant impacts globally (IPCC 2013, 2021) including southern Africa (Engelbrecht et al. 2015; Maúre et al. 2018; Almazroui et al. 2020). In this southern Africa region lies the Okavango River Basin (ORB; Fig. 1) focused on in the present study, which, like most of the sub-continent, is affected by large climate variability which is likely to be worsened by climate change (Andersson et al. 2003; Wolski and Murray-Hudson 2008). The ORB, stretching from Angola through Namibia to Botswana, contains the world-famous Okavango Delta located in the latter country. The Delta is a world heritage and Ramsar site famous for its highly biodiverse and sensitive ecosystems (Murray-Hudson et al. 2006; UNESCO 2014) supporting economically vital ecotourism (Mbaiwa 2004, 2015). These ecosystems crucially depend on the highly seasonal ORB streamflow, which is also a critically important source of freshwater for the rural population, most of whom rely on rain-fed subsistence farming like over the bulk of southern Africa (McCarthy et al. 2003; Andersson et al. 2003, 2006; Kgathi et al. 2006; Murray-Hudson et al. 2006; Moses and Hambira 2018).

The large climate variability impacts rain-fed subsistence farming and water availability (Tyson 1986; Reason et al. 2006; Murray-Hudson et al. 2006; Conway et al. 2015; Moses and Hambira 2018) as well as wildlife distribution and tourism (Mbaiwa 2004, 2015; Murray-Hudson et al. 2006). It is worth noting that clearing of vegetation over large areas for farming and potential oil mining in the ORB region (Richardson 2021) could cause widespread ecological disruption. Factors contributing to the mentioned large climate variability are complex, with the El Niño-Southern Oscillation (ENSO) in the tropical Pacific being the main interannual climate mode affecting the region (Lindesay 1988; Reason et al. 2000; Reason and Jagadheesha 2005; Blamey et al. 2018; Hart et al. 2018; Moses et al. 2022). Recurring climate extremes such as droughts, hot days and floods brought about by extreme rainfall events are common (e.g., Tyson 1986; Reason

✉ O. Moses
   omoses@ub.ac.bw

1   Okavango Research Institute, University of Botswana, Maun, Botswana
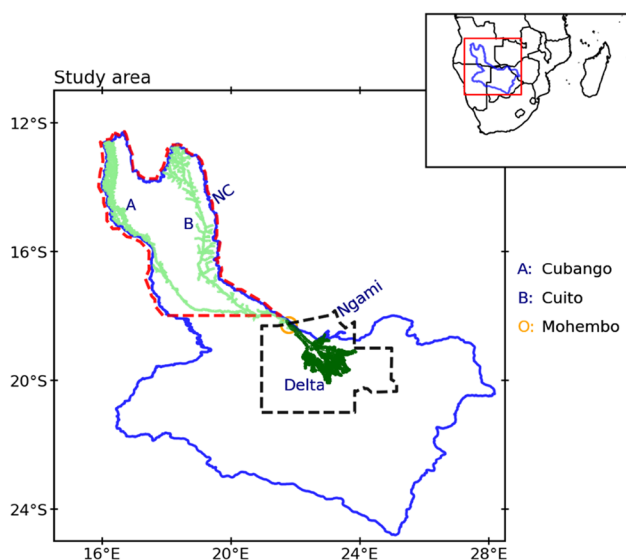
Fig. 1 The Okavango River Basin (ORB), i.e., the blue polygon within the box 11–25°S, 14.5–28.5°E, with its location in southern Africa shown in the insert. "A" and "B" within the ORB denote the two main rivers, namely, the Cubango and Cuito, respectively, which merge to form the Okavango River which then feeds into the Okavango Delta through Mohembo hydrological station (orange circle). The ORB is also subdivided into the north catchment (red dashed polygon denoted by "NC") and Ngamiland (black dashed polygon denoted by "Ngami")

et al. 2006; Meque et al. 2022; Moses et al. 2023a, 2023b), and their intensities and frequencies are likely to increase over the region due to global warming (IPCC 2013, 2021). Changes in the climate are also associated with tropical diseases such as schistosomiasis (Gabaake et al. 2023).

Temperatures are generally high particularly in the Botswana part of the ORB, which may worsen the impacts of severe drought for example (Moses 2017; Moses and Gondwe 2019; Moses et al. 2022). Rainfall occurs mainly during October to March or April, with the Botswana/Namibian (Angolan) part of the basin having a semi-arid (subtropical) climate. Moses et al. (2023a) found significant drying and warming trends over the ORB and most of southern Africa particularly in the early summer (October–November) during the period 1981–2021. These trends are consistent with warming (Barros and Field 2014; Engelbrecht et al. 2015; Maúre et al. 2018; Meque et al. 2022) and early summer drying (IPCC 2021; Munday and Washington 2019; Wainwright et al. 2021) found over southern Africa. If these trends persist, they may have adverse impacts on rain-fed subsistence farming (Guilpart et al. 2017), water availability and ecosystems (Murray-Hudson et al. 2006). Decreases in rainfall combined with increases in temperature may increase soil moisture losses which may limit crop growth.

While relatively more studies have considered rainfall and temperature characteristics for the recent past over the ORB region or over southern Africa, relatively limited research has been done on future characteristics of these variables over the former region. Some of the above-mentioned studies like Wainwright et al. (2021) considered future rainfall characteristics over southern Africa more generally, not necessarily specifically over the ORB region, based on the Coupled Model Intercomparison Project Phase 6 (CMIP6; Eyring et al. 2016). They found delays in the wet seasons of up to 2 weeks by the end of the twenty-first century across southern Africa. Others like Almazroui et al. (2020) also used CMIP6 models to examine future changes in rainfall and temperature over Africa as a whole and over eight subregions which included southwest Africa (southern Africa landmass west of 26°E longitude and south of 10°S latitude). These authors considered future changes in rainfall and temperature on annual scales and specifically for the boreal winter (December-February) and boreal summer (July–August). They found large spatial variability in rainfall, and significant warming which varied regionally, but changes in the variables over the ORB region were not significantly addressed. Lim Kam Sian et al. (2021) considered changes in rainfall in the twenty-first century over southern Africa using regional demarcations like those used by Almazroui et al. (2020). Focusing on December-March and May–October, Lim Kam Sian et al. (2021) found that rainfall trends over large regions cannot be generalised, hence recommended localised studies to provide more accurate findings.

The principal aim of this study is to analyse future (up to the end of the twenty-first century) changes in rainfall and temperature using CMIP6 models over the ORB region, focusing on the extended rainy season October–April (months during which most crops are grown), split into October–November (ON), December-February (DJF) and March–April (MA), as explained further in Section 2. Due to the massive improvements of the CMIP6 compared to previous CMIP projects (Eyring et al. 2016), CMIP6 models are expected to give more reliable results as shown by previous studies (Mauritsen et al. 2019; Moseid et al. 2020), hence these models are used in the present study. Given the vulnerability of the ORB region and the dependency of the local population on rain-fed subsistence farming, the results of the study may help improve the management of agricultural activities, water resources and the highly biodiverse ecosystems. Improved management is critical for sustainable use of the ORB resources.

2 Data and methods

The study area is the ORB and its selected two subregions, namely, the north catchment and Ngamiland (Fig. 1). The former subregion is where most of the ORB streamflow is

generated and the latter subregion contains the world-famous Okavango Delta, where most of the streamflow terminates (Andersson et al. 2003; Wolski and Murray-Hudson 2008; Moses et al. 2023a, 2023b). Due to lack of high-resolution observational data in the study area, the 0.05° resolution Climate Hazards Infrared Rainfall with Station data (CHIRPS; Funk et al. 2015) version 2, and the 2-m air temperature (T2m) from 0.25° resolution ERA5 reanalyses (Copernicus Climate Change Service 2017; Hersbach et al 2020), were analysed to depict the annual cycles and climatologies of rainfall and temperature. These CHIRPS and ERA5 T2m data have been found to agree well with station data (Moses et al. 2022; Moses 2023). To be in line with the Intergovernmental Panel on Climate Change Sixth Assessment Report (IPCC 2021), which is based on CMIP6 models, ERA5 T2m and CHIRPS annual cycles and climatologies were analysed for the period 1985–2014, taken to be the historical period. The climatologies were analysed for ON, DJF and MA, based on previous analyses for rainfall over the ORB (Moses et al. 2022, 2023a) and for dry spells over southern Africa (Thoithi et al. 2021). Very little rain occurs in the ORB during May–September. Typically, December to February are the wettest months, hence the main growing season. Some years also experience significant falls in ON (onset of the rainy season) or March–April (end of the rainy season).

In addition, CHIRPS and ERA5 T2m data were used to evaluate the performance of the selected CMIP6 models (discussed later in this section) in reproducing the observed annual cycles of rainfall and temperature over the study area, and to evaluate the performance of these models in reproducing the observed interannual variability in rainfall and temperature changes during the historical period, focusing on ON, DJF and MA, for the same reasons as above. For the performance evaluation, model historical simulations were used. The metrics used included the bias, root-mean-square-error (RMSE) and correlations, which have also been used in previous studies (Almazroui et al. 2020; Ayugi et al. 2021; Xu et al. 2021; Jamal et al. 2023). Biases and RMSEs close to zero indicate that model data are close to the observations. A correlation of -1 represents an opposite relationship, 0 means no correlation, and 1 represents a perfect correlation.

Based on the results of the model performance evaluation and on previous studies (Xu et al. 2021; Jamal et al. 2023) that model projections without bias correction are highly uncertain, in the present study model projections were bias corrected using the mean bias correction method (Holland et al. 2010; Bruyère et al. 2014). This method was applied to model outputs for the historical period (1985–2014) and for the selected future periods, i.e., 2030–2059 (near term) and 2070–2099 (long term), so that the difference between projections for the future and historical periods is a result and signal for climate change in the seasons (ON, DJF, ON) of interest. The mean bias correction method was applied to

rainfall and temperature simulations based on Eqs. 1 and 2, respectively.

$$\text{Corr sim RN} = \text{uncorrected sim RN}/(\text{mean observed RN}/\text{mean sim RN}) \tag{1}$$

$$\text{Corr sim T} = \text{uncorrected sim T} - (\text{mean sim T} - \text{mean observed T}) \tag{2}$$

where corr, sim, RN and T denote corrected, simulated, rainfall and temperature, respectively.

The CMIP6 models that were used in this study were the CESM2-WACCM (Danabasoglu 2019) (hereafter, CESM), CMCC-CM2-SR5 (Lovato and Peano 2020) (hereafter, CMCC), MPI-ESM1-2-HR (Schupfner et al. 2019) (hereafter, MPI), and the average of these models (hereafter, model average). Selection of these models was based on the available computer resources used to perform the analyses, downloadability (dependent on internet connectivity) of historical and projected model outputs, as well as on relatively high model grid resolutions. The CESM and CMCC models have resolutions (longitude x latitude) of 1.25°×0.94° each, whereas the MPI model has a resolution of 0.94°×0.94°. These models were re-gridded to a common grid of lowest model resolution using linear re-gridding scheme. The first realization (r1i1p1f1) for each model was used in the analysis. The model projections were analysed under two shared socioeconomic pathways (SSPs; Gidden et al. 2019), namely, SSP245 and SSP585. SSP585 is the highest emission scenario and the SSP245 scenario represents a medium emission scenario (Van Vuuren et al. 2011; O'Neill et al. 2016).

Trends in rainfall and temperature changes were considered. They were tested for statistical significance at the 95% confidence level, using the Hamed and Rao (1998) and Yue and Wang (2002) tests. Both tests are modified from the nonparametric Mann–Kendall test (MKT) (Mann 1945; Kendall 1975), which is widely used because it exempts datasets from normal distribution requirements and is less sensitive to outliers. However, unlike the modified trend tests used in the present study, the original MKT does not take data autocorrelation into consideration.

3 Results and discussion

3.1 Observed climatology and model performance

Figures 2a-c show the observed rainfall climatology over the ORB in ON, DJF and MA, for the historical period. In all three seasons, the north catchment receives more rainfall than Ngamiland (see Fig. 1 for locations). This is consistent with Moses et al. (2023b) who found the former region to experience more extreme rainfall events than the latter

region during their study period (1981–2021). The main contributors to high rainfall over the former region include the Angola Low and orographic uplift (Munday and Washington 2017; Moses et al. 2022). Figures 2a-c also show that most of the rainfall occurs in DJF, with the northern part of the north catchment receiving 7–8 mm/day, and the southern part of Ngamiland receiving 2–3 mm/day. Although MA experiences less rainfall than DJF, it generally experiences more rainfall than ON. The observed temperature

climatology over the ORB in ON, DJF and MA, for the historical period is shown in Figs. 3a-c. Most parts of the ORB including Ngamiland and the southern parts of the north catchment, experience largest temperatures (seasonal mean of 26–28 °C) in ON, which is also relatively drier compared to the other two seasons as already mentioned. The southern parts of Ngamiland also experience the same range of temperatures in DJF. Overall, over the ORB, the lowest temperatures (16–18 °C) in all three seasons occur over the northern
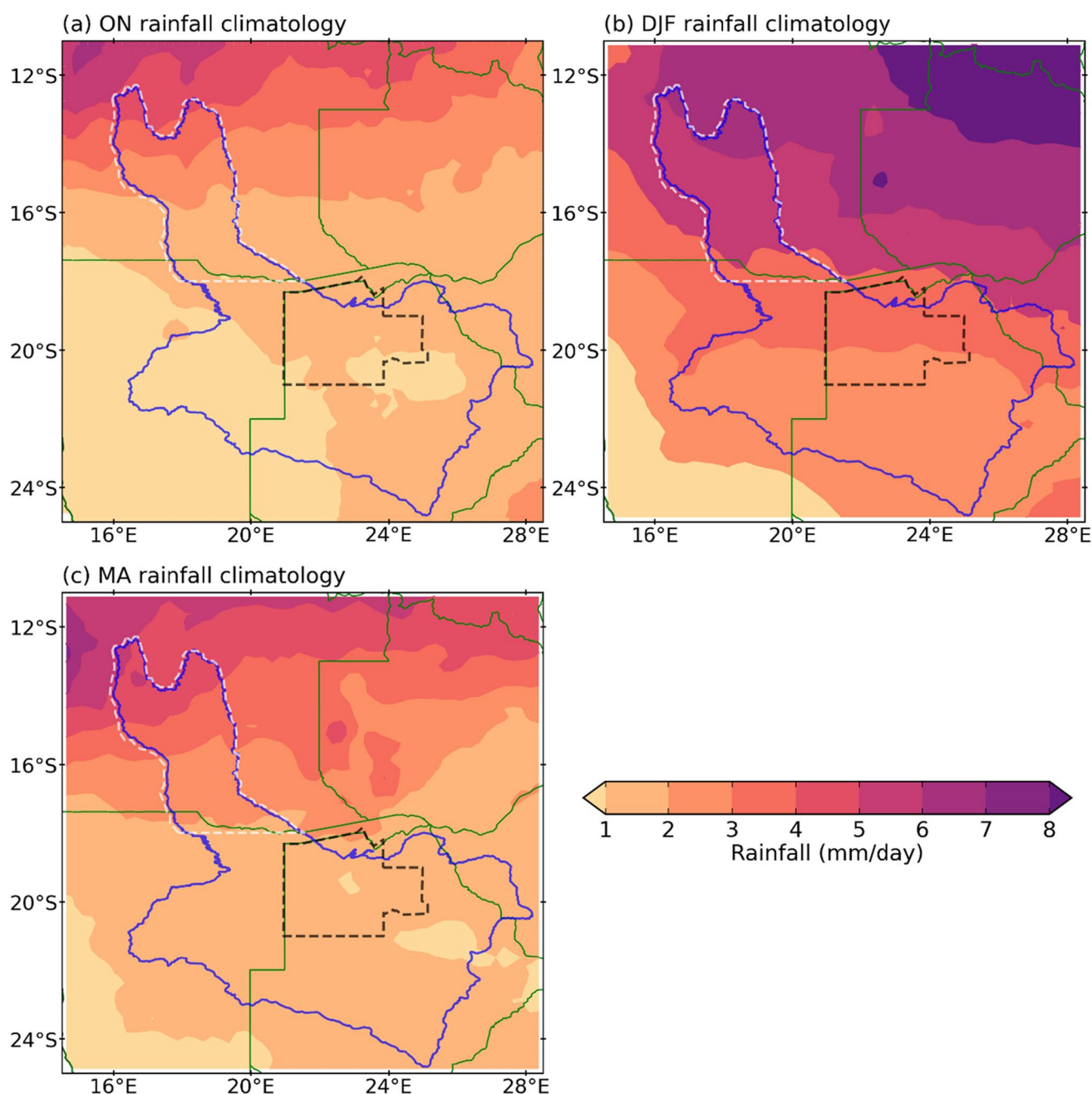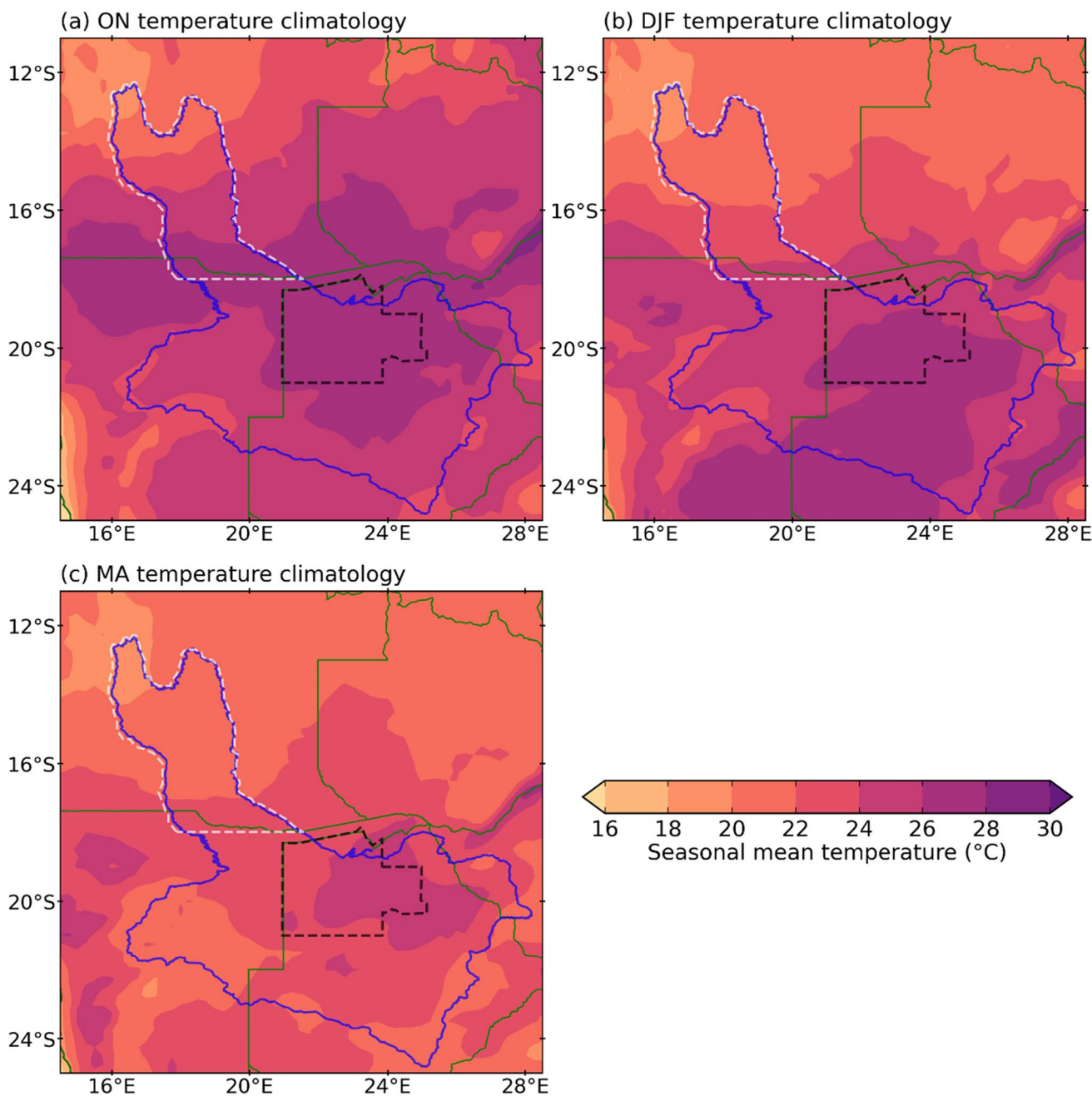

Fig. 2 Observed rainfall climatology (based on CHIRPS) over the ORB, for (a) ON, (b) DJF and (c) MA, 1985–2014. The ORB and its subdivisions are described in Fig. 1

parts of the north catchment and the highest temperatures (26–28 °C) occur over Ngamiland. Occurrence of highest temperatures over Ngamiland is in harmony with previous studies (Moses and Gondwe 2019; Moses et al. 2022).

The performance of historical simulations from the CMIP6 models in reproducing the observed rainfall annual cycle for the historical period over the north catchment and Ngamiland is shown in Figs. 4a-b. Note that the climatological year is defined as starting from July and ending in June

the following year to capture the full austral summer rainfall period (October–April) as a single season (Maruatona and Moses 2022). The figure shows that over both regions, all the models (CESM, CMCC, MPI and the model average) generally overestimate the observed rainfall annual cycle. The performance of the models is consistent with other studies over southern Africa (Lim Kam Sian et al. 2021), over Africa as a whole (Almazroui et al. 2020) and elsewhere (Ayugi et al. 2021; Liang-Liang et al. 2022). It is noted that


Fig. 3 Observed temperature climatology (based on ERA5 T2m) over the ORB, for (**a**) ON, (**b**) DJF and (**c**) MA, 1985–2014. The ORB and its subdivisions are described in Fig. 1

rainfall values for the north catchment are larger than those for Ngamiland (Figs. 4a-b), consistent with Fig. 2. The wettest months over both regions are November-March and the driest ones are May–September (Figs. 4a-b), consistent with previous authors (Moses et al. 2022). Considerable amount of rainfall also occurs in October and April.

Figures 4c-d show the performance of the models (historical simulations) in reproducing the observed temperature annual cycle for the historical period over the north catchment and Ngamiland. Over both regions, temperatures reach their minimums in July, increase sharply thereafter until they reach their peak in October before dropping again. As found for rainfall, the models generally overestimate the observed temperature annual cycle. Over Ngamiland, the exception is in January-March (December) when the MPI (CMCC) underestimate this annual cycle. Over the north catchment, the CESM and the model average generally overestimate this annual cycle except in July–September whereas the CMCC overestimates it in all the months. It is only the MPI that generally underestimates the observed temperature annual cycle except in October-December. Ayugi et al. (2021) suggested that model overestimations maybe related to equilibrium climate sensitivity.
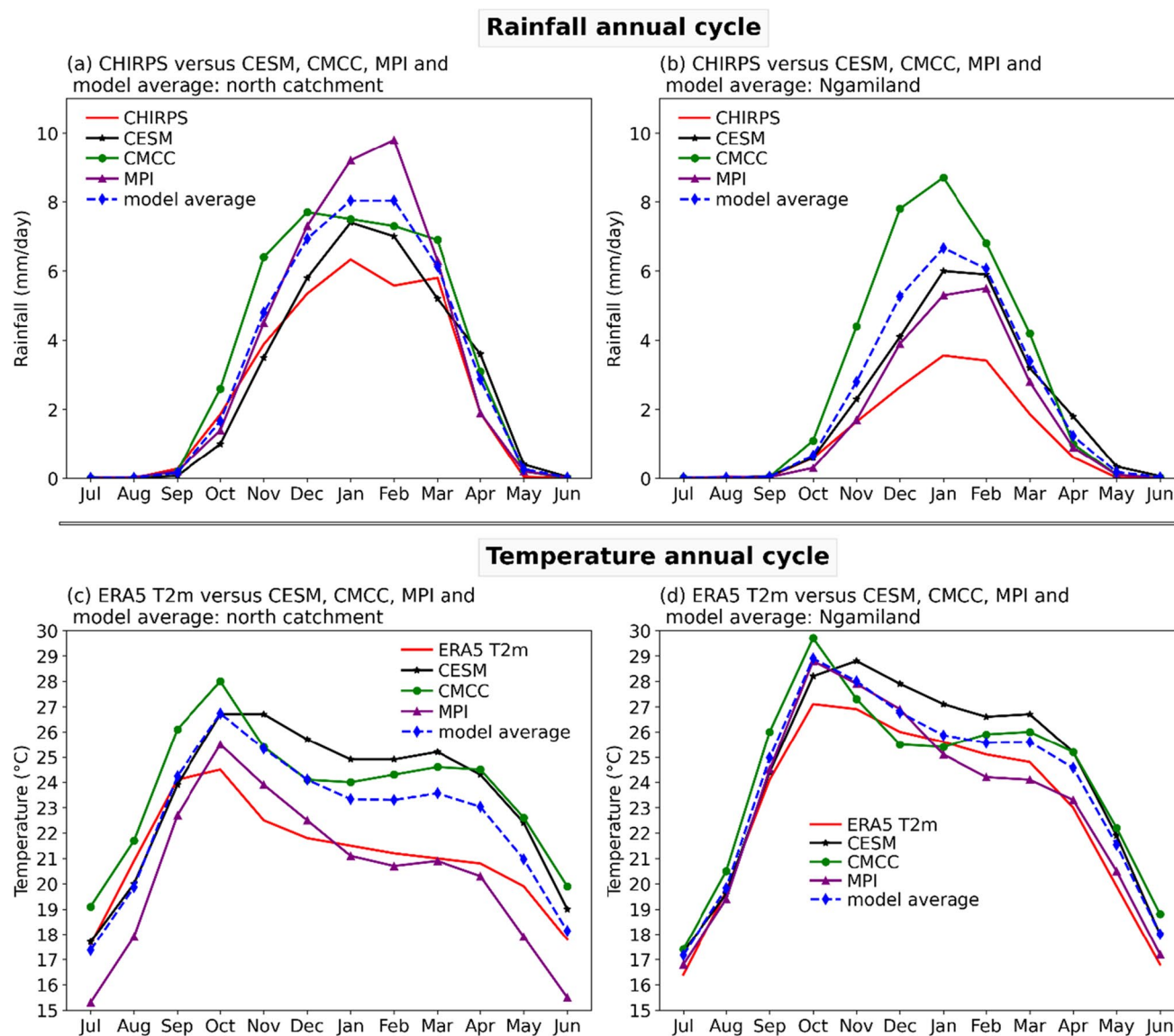
Fig. 4 (**a**) Annual cycle of rainfall over the north catchment based on historical (1985–2014) simulations from the CMIP6 models (CESM, CMCC, MPI, model average) compared with observations (CHIRPS). (**b**) As in (a) but for Ngamiland. (**c**) Annual cycle of temperature over the north catchment based on historical simulations from the CMIP6 models compared with observations (ERA5 T2m). (**d**) As in (c) but for Ngamiland. Locations of the north catchment and Ngamiland are shown in Fig. 1
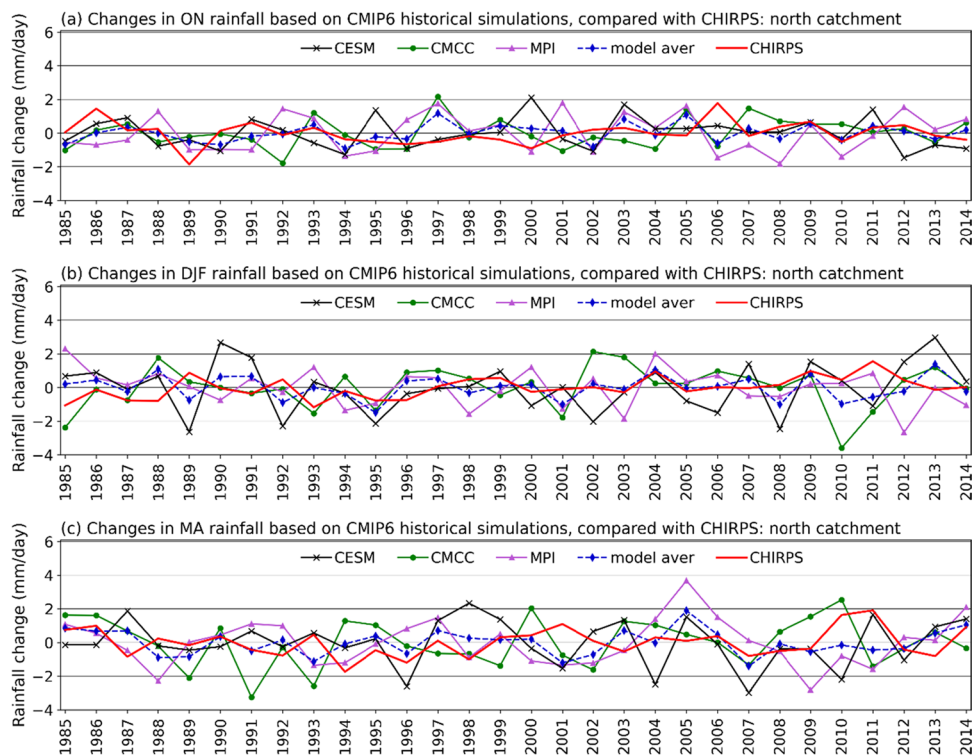
Figure 5 shows the performance of the models (historical simulations) in reproducing the observed interannual variability in rainfall changes over the north catchment. Generally, the performance of the models is fair. It is worth noting that in ON during some years like 1985–1986 and 2006 (1989 and 1999), all the models including the model average underestimate (overestimate) the observed interannual variability in rainfall changes (Fig. 5a). Compared with the individual models, the model average resembles the observed interannual variability better (Figs. 5a-c). Previous authors noted that model average reduces biases by partly cancelling them out (Pincus et al. 2008; Ayugi et al. 2021). Figure 6 is as Fig. 5, but for Ngamiland. As found for the north catchment, the performance of the historical simulations from the models in reproducing the observed interannual variability in rainfall changes is also fair over Ngamiland. The individual models and the model average resemble the observed variability better in ON (Fig. 6a) than in DJF and MA (Figs. 6b-c).

The performance of the models (historical simulations) in reproducing the observed interannual variability in temperature changes over the north catchment is shown in Fig. 7. Generally, the models fairly reproduce the observed interannual variability. As found for rainfall, the model average shows a better resemblance of the observed interannual variability in temperature changes than the individual models. Also, as found for rainfall, the models including the model average overestimate (underestimate) the observed variability during some years such as DJF 2011–2013 (DJF
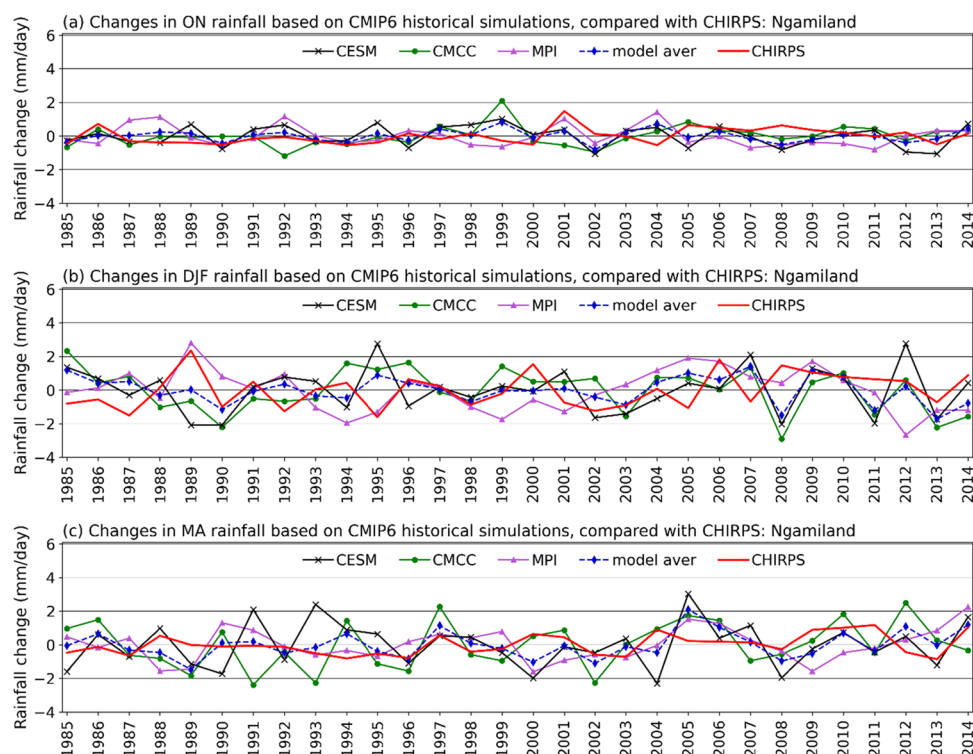
1987–1988), as can be seen mainly in Fig. 7b. Figure 8 is as Fig. 7 but for Ngamiland. The interannual variability in temperature changes is larger over Ngamiland than over the north catchment. As in the case for the north catchment, the individual models and the model average overestimate (underestimate) the observed interannual variability in temperature changes over Ngamiland during some years like 2011–2014 (1998–1999), which is clearer in Fig. 8b (Fig. 8c).

The computed biases (Table 1), which are generally positive, suggest that historical simulations from the models generally overestimate the observed interannual variability in temperature changes (Figs. 7 and 8). There are only a few cases where the models underestimate (negative biases) the observed interannual variability in temperature changes, such as in MA when the MPI biases are -0.31 °C over the north catchment and -0.18 °C over Ngamiland (Table 1). Similarly, rainfall biases (Table 1) suggest that historical simulations from the models mainly overestimate the observed interannual variability in rainfall changes (Figs. 5 and 6). It is only in ON when the CESM and MPI underestimate the observed interannual variability in rainfall changes, with these models showing biases of -0.62 mm/day (over the north catchment) and -0.10 mm/day (over Ngamiland), respectively (Table 1). Although the models' historical simulations generally overestimate the observed interannual variability in rainfall and temperature changes (Table 1), RMSEs (Table 2) suggest that overall, the performance of models (Figs. 5–8) is fair since
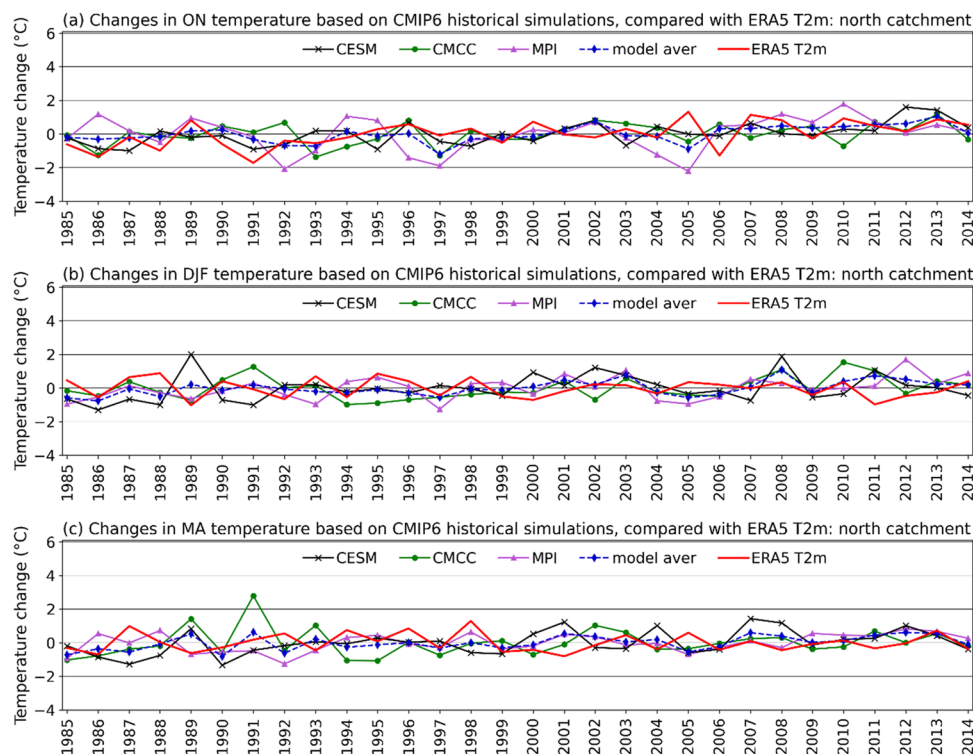
Fig. 5 (**a**) Changes in rainfall over the north catchment based on historical (ON 1985–2014) simulations from the CMIP6 models [CESM, CMCC, MPI, model average (aver)] compared with observations (CHIRPS). (**b**) As in (a) but for DJF. DJF 1985 means December 1985 to February 1986, and so on. (**c**) As in (a) but for MA. Location of the north catchment is shown in Fig. 1

Fig. 6 As in Fig. 5 but for Ngamiland, whose location is shown in Fig. 1

(a) Changes in ON rainfall based on CMIP6 historical simulations, compared with CHIRPS: Ngamiland

(b) Changes in DJF rainfall based on CMIP6 historical simulations, compared with CHIRPS: Ngamiland

(c) Changes in MA rainfall based on CMIP6 historical simulations, compared with CHIRPS: Ngamiland

Fig. 7 (**a**) Changes in temperature over the north catchment based on historical (ON 1985–2014) simulations from the CMIP6 models [CESM, CMCC, MPI, model average (aver)] compared with observations (ERA T2m). (**b**) As in (a) but for DJF. DJF 1985 means December 1985 to February 1986, and so on. (**c**) As in (a) but for MA. Location of the north catchment is shown in Fig. 1

(a) Changes in ON temperature based on CMIP6 historical simulations, compared with ERA5 T2m: north catchment

(b) Changes in DJF temperature based on CMIP6 historical simulations, compared with ERA5 T2m: north catchment

(c) Changes in MA temperature based on CMIP6 historical simulations, compared with ERA5 T2m: north catchment

these errors are generally low over both the north catchment and Ngamiland, with those for temperature (rainfall) ranging from 0.77 to 4.00 °C (0.79 to 3.29 mm/day) in all three seasons. Correlations between the observed and simulated (historical) interannual variability in rainfall and temperature changes (Figs. 5–8) were generally weak, except for those between the CESM temperature and ERA5 T2m in ON, which were positive and significant over both the north catchment and Ngamiland (0.35 over both regions).

Fig. 8 As in Fig. 7 but for Ngamiland, whose location is shown in Fig. 1
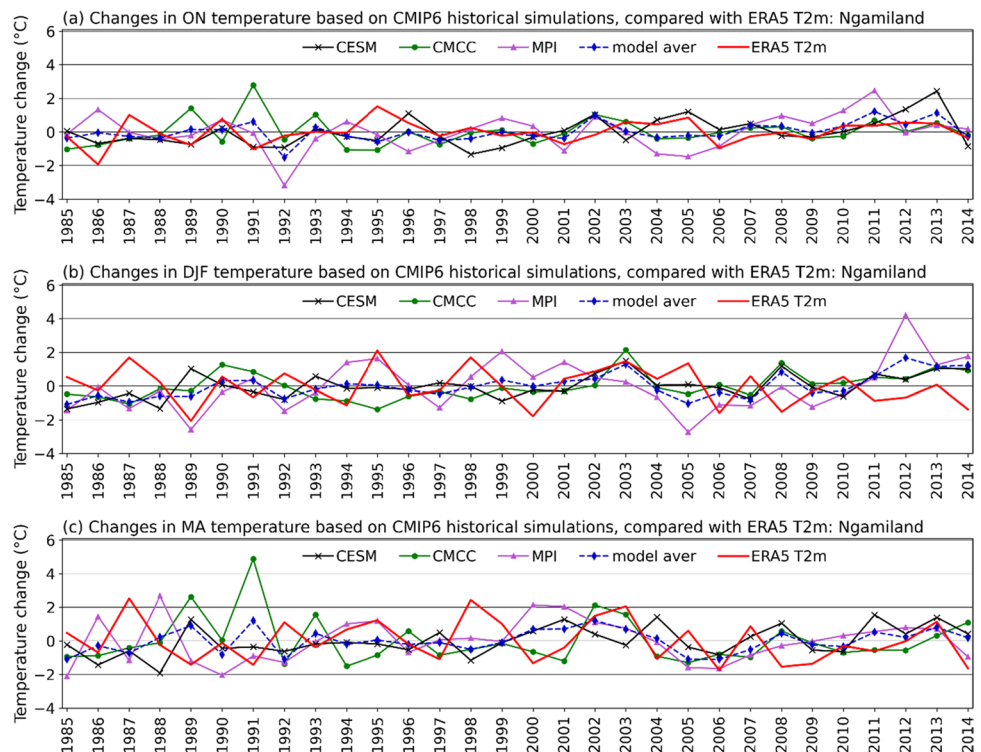
Table 1 Biases of temperature (in °C) and rainfall (in mm/day) from historical simulations of CMIP6 models [CESM, CMCC, MPI, model average (aver)] compared with observations (ERA5 T2m and CHIRPS) over the north catchment and Ngamiland, in ON, DJF and MA, 1985–2014. The biases have been computed from seasonal fields

Biases		North catchment		Ngamiland	
Season	Model	ERA5 T2m	CHIRPS	ERA5 T2m	CHIRPS
ON	CESM	3.13	-0.62	1.46	0.32
	CMCC	3.12	1.60	1.51	1.64
	MPI	1.08	0.07	1.35	-0.10
	model aver	2.44	0.35	1.44	0.62
DJF	CESM	3.68	1.04	1.61	2.16
	CMCC	2.63	1.80	-0.03	4.59
	MPI	-0.05	3.12	-0.22	1.76
	model aver	2.09	1.99	0.45	2.84
MA	CESM	3.87	0.50	2.05	1.25
	CMCC	3.64	1.18	1.68	1.39
	MPI	-0.31	0.26	-0.18	0.61
	model aver	2.40	0.65	1.18	1.08

Table 2 RMSEs of temperature (in °C) and rainfall (in mm/day) from historical simulations of CMIP6 models [CESM, CMCC, MPI, model average (aver)] compared with observations (ERA5 T2m and CHIRPS) over the north catchment and Ngamiland, in ON, DJF and MA, 1985–2014. The RMSEs have been computed from seasonal fields

RMSEs		North catchment		Ngamiland	
Season	Model	ERA5 T2m	CHIRPS	ERA5 T2m	CHIRPS
ON	CESM	3.23	1.21	1.69	0.84
	CMCC	3.26	1.95	1.91	1.80
	MPI	1.62	1.32	1.85	0.79
	model aver	2.57	0.91	1.68	0.86
DJF	CESM	3.84	1.92	2.15	2.84
	CMCC	2.75	2.26	1.45	1.81
	MPI	0.83	3.39	1.88	2.27
	model aver	2.22	2.21	1.48	3.15
MA	CESM	4.00	1.65	2.64	1.89
	CMCC	3.77	1.97	2.62	1.92
	MPI	0.77	1.60	1.70	1.31
	model aver	2.51	1.27	1.92	1.41

Based on the results of model performance evaluation, the model outputs were bias corrected using the method described in Section 2. The bias corrected model outputs were used in the next section to analyse future climate projections over the study area.

3.2 Future climate projections

3.2.1 Rainfall projections

Figure 9 shows bias corrected future projections (up to the end of the twenty-first century) of changes in rainfall under the SSP245 and SSP585 scenarios over the north catchment.

Generally, all the models including the model average show a mixture of increases and reductions in average rainfall during the future periods [near term (2030–2059) and long term (2070–2099)]. For the near term period under the SSP585 (SSP245) scenario, the CESM projects average rainfall changes of 0.12 mm/day (0.06 mm/day), -0.11 mm/day (0.06 mm/day) and -0.02 mm/day (0.02 mm/day), in ON, DJF and MA, respectively, whereas for the long term period, it projects 0.18 mm/day (0.11 mm/day), -0.11 mm/day (-0.03 mm/day) and -0.02 mm/day (-0.03 mm/day). The CMCC under the SSP585 (SSP245) scenario, for the near term period projects average rainfall changes of -0.09 mm/day (-0.07 mm/day), 0.01 mm/day (-0.00 mm/day) and -0.01 mm/day (-0.01 mm/day), in ON, DJF and MA, respectively, whilst for the long term period, it projects -0.13 mm/day (-0.13 mm/day), 0.02 mm/day (-0.19 mm/day) and -0.00 mm/day (0.00 mm/day). The MPI under the SSP585 (SSP245) scenario, for the near term period, projects average rainfall changes of 0.12 mm/day (0.04 mm/day), 0.14 mm/day (-0.13 mm/day) and 0.06 mm/day (0.04 mm/day), in ON, DJF and MA, respectively, whereas for the long term period, it projects 0.20 mm/day (0.21 mm/day), 0.18 mm/day (0.12 mm/day) and 0.11 mm/day (0.11 mm/day). For the model average during the near term period under the SSP585 (SSP245) scenario, it projects average rainfall changes of 0.05 mm/day (0.01 mm/day), 0.01 mm/day (-0.02 mm/day) and 0.01 mm/day (0.02 mm/day), whilst for the long term period, it projects 0.08 mm/day (0.06 mm/day), 0.03 mm/day (0.02 mm/day) and 0.03 mm/day (0.02 mm/day). Overall,

the models project larger variability in rainfall changes in DJF than in ON and MA.

Bias corrected rainfall projections for Ngamiland are shown in Fig. 10. Under the SSP245 scenario in ON during the near term period, the CESM, CMCC, MPI and the model average project average rainfall changes of 0.15 mm/day, 0.44 mm/day, 0.00 mm/day and 0.20 mm/day, respectively, whereas for the long term period these models project 0.18 mm/day, 0.75 mm/day, 0.04 and 0.33 mm/day, respectively. The changes in DJF and MA rainfall (Figs. 10b-c) over Ngamiland are larger than those projected over the north catchment (Figs. 9b-c), whereas in ON, the changes are larger over the north catchment (Fig. 9a) than over Ngamiland (Fig. 10a). This difference in spatial distribution of rainfall changes over the two regions is consistent with Almazroui et al. (2020) who found large variability in rainfall changes over Africa during the twenty-first century. Over both Ngamiland and the north catchment, projected rainfall changes under the SSP245 scenario cannot be generalised to be larger or smaller than those projected under the SSP585 scenario.

Some significant decreasing trends have been found in the projected rainfall changes over Ngamiland, but none were significant over the north catchment. During the near term period those significant trends are projected by the CESM, MPI and the model average, with trend magnitudes of -63.90 mm/decade (in DJF under SSP245), -28.20 mm/decade (in MA under SSP245) and -30.60 mm/decade (in MA under SSP585), respectively. During the long term period,

Fig. 9 (**a**) Changes in rainfall over the north catchment based on CMIP6 model [CESM, CMCC, MPI, model average (aver)] projections for the future (ON 2030 to 2099), under SSP245 and SSP585 scenarios. CESM_ssp245 means CESM projection under the SSP245 scenario, and so on. Model aver ssp245 (ssp585) means model average under the SSP245 (SSP585) scenario. (**b**) As in (a) but for DJF. DJF 1930 means December 1930 to February 1931, and so on. (**c**) As in (a) but for MA. Location of the north catchment is shown in Fig. 1
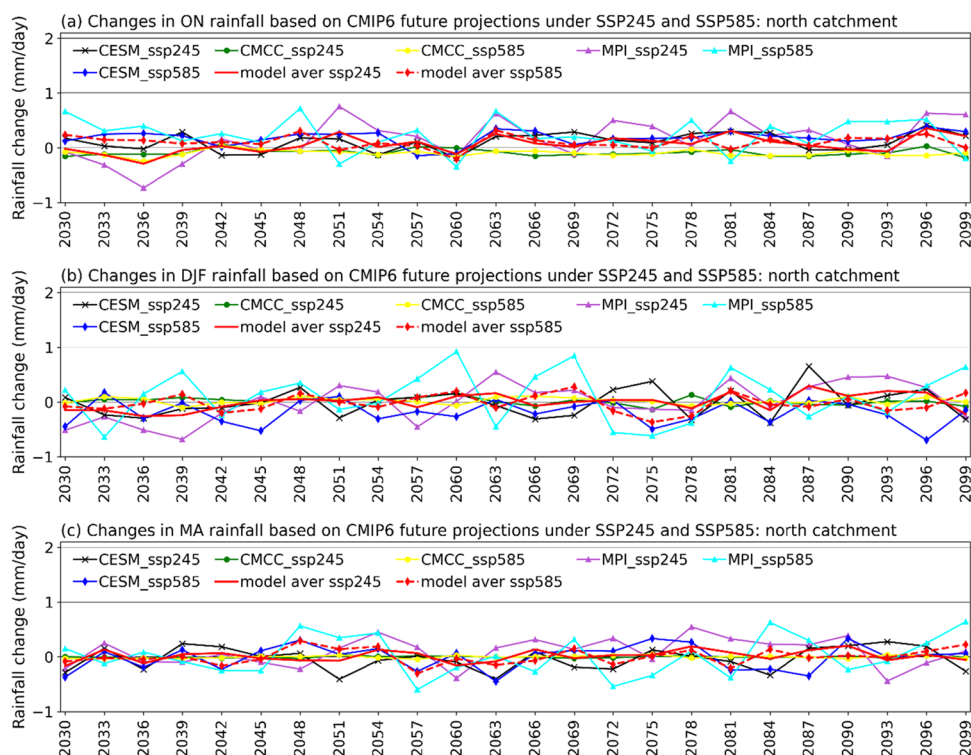
Fig. 10 As in Fig. 9 but for Ngamiland, whose location is shown in Fig. 1
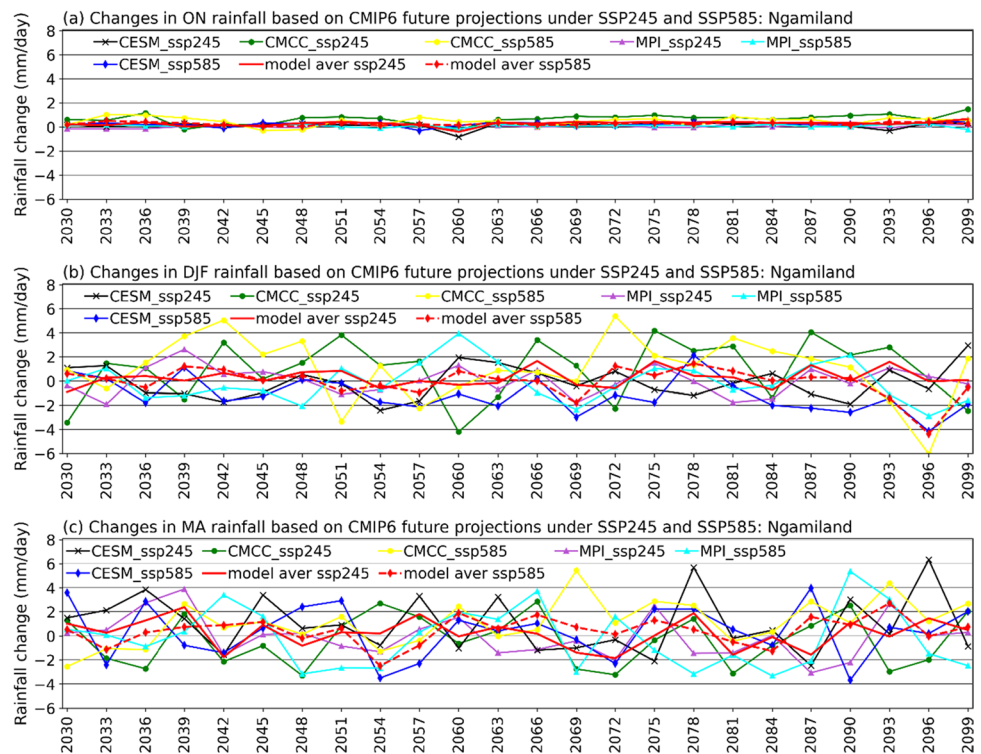
it is only in DJF under the SSP585 scenario that the models project significant decreasing trends over Ngamiland, with the CESM, CMCC, MPI and the model average projecting -49.50 mm/decade, -87.20 mm/decade, -74.70 mm/decade and -85.50 mm/decade, respectively. The significant decreasing trends in the projected rainfall changes are consistent with previous studies (Almazroui et al. 2020; Lim Kam Sian et al. 2021). It is worth noting that for the nonsignificant trends over both Ngamiland and the north catchment, some were negative while others were positive.

3.2.2 Temperature projections

Figure 11 shows bias corrected future projections (up to the end of the twenty-first century) of changes in temperature under the SSP245 and SSP585 scenarios over the north catchment. Considering the projections for the long term period first, the figure shows that under the SSP585 (SSP245) scenario the CESM projects average warming values of 6.20 °C (3.54 °C), 5.90 °C (3.25 °C) and 5.37 °C (2.77 °C), in ON, DJF and MA, respectively. For the same long term period, the CMCC under the SSP585 (SSP245) scenario projects 6.04 °C (4.18 °C), 3.92 °C (2.09 °C) and 3.84 °C (2.18 °C), in ON, DJF and MA, respectively. The MPI projects smaller warming values than both the CESM and CMCC, i.e., under the SSP585 (SSP245) scenario it projects 3.84 °C (2.88 °C), 3.28 °C (2.00 °C) and 3.84 °C (2.16 °C), in ON, DJF and MA, respectively. For the same seasons, the model average under the SSP585 (SSP245)

scenario projects average warming values of 5.36 °C (3.53 °C), 4.37 °C (2.44 °C) and 4.35 °C (2.37 °C). Paying attention to the near term period in Fig. 11, under the SSP585 (SSP245) scenario the CESM projects average warming values of 2.71 °C (2.10 °C), 2.51 °C (1.82 °C) and 2.03 °C (1.88 °C), in ON, DJF and MA, respectively, which are larger than those projected by the CMCC [2.65 °C (2.04 °C), 1.56 °C (1.00 °C), 1.70 °C (1.13 °C)], MPI [1.91 °C (1.33 °C), 1.52 °C (0.75 °C), 1.61 °C (1.17 °C)] and the model average [2.42 °C (1.82 °C), 1.86 °C (1.19 °C), 1.78 °C (1.39 °C)]. Overall, Fig. 11 shows that all the models project a larger warming during the long term period than during the near term period.

Figure 12 shows bias corrected temperature projections for Ngamiland. For the long term period under the SSP585 (SSP245) scenario, the CESM projects average warming values of 6.71 °C (3.76 °C), 7.02 °C (3.64 °C) and 6.06 °C (2.84 °C), in ON, DJF and MA, respectively, which are overall larger than those projected by the CMCC [6.23 °C (4.36 °C), 4.05 °C (2.67 °C), 3.95 °C (2.36 °C)], MPI [4.42 °C (2.64 °C), 3.83 °C (2.22 °C), 4.41 °C (2.72 °C)] and the model average [5.78 °C (3.59 °C), 4.96 °C (2.84 °C), 4.81 °C (2.64 °C)]. For the near term period the CESM again projects larger warming than the other models, but with smaller warming values during this period than during the long term period as in the case for the north catchment. Overall, the projected average warming over Ngamiland (Fig. 12) is larger than that projected over the north catchment (Fig. 11). Over both regions,

Fig. 11 (**a**) Changes in temperature over the north catchment based on CMIP6 model [CESM, CMCC, MPI, model average (aver)] projections for the future (ON 2030 to 2099) under SSP245 and SSP585 scenarios. CESM_ssp245 means CESM projection under the SSP245 scenario, and so on. Model aver ssp245 (ssp585) means model average under the SSP245 (SSP585) scenario. (**b**) As in (a) but for DJF. DJF 1930 means December 1930 to February 1931, and so on. (**c**) As in (a) but for MA. Location of the north catchment is shown in Fig. 1
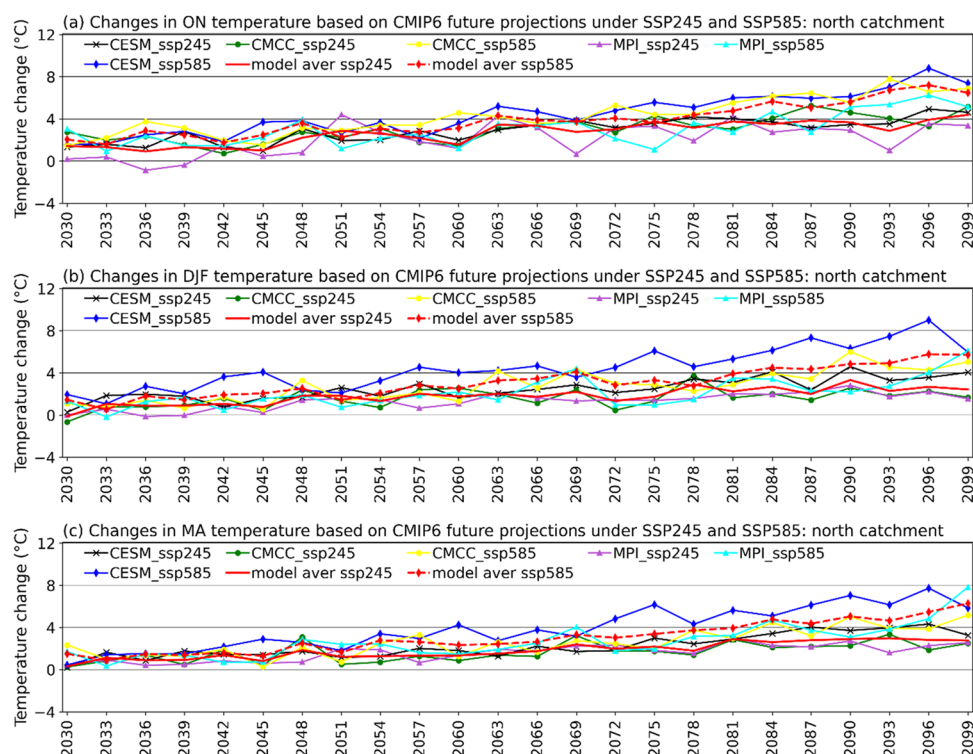
Fig. 12 As in Fig. 11 but for Ngamiland, whose location is shown in Fig. 1
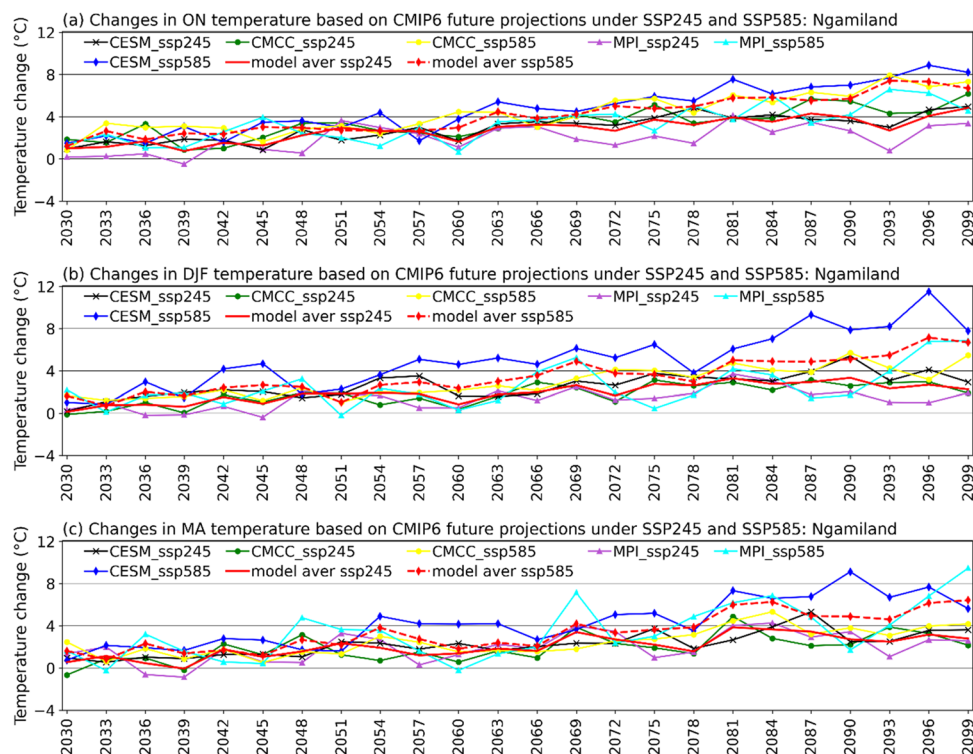
unsurprisingly, the warming projected under the SSP585 scenario is larger than that projected under the SSP245 scenario. This is consistent with Almazroui et al. (2020) who, over Africa, projected mean annual temperature increases during the near term (long term) period of 1.5 °C

(2.3 °C) and 1.8 °C (4.4 °C) under the SSP245 and SSP585 scenarios, respectively. The SSP245 and SSP585 represent medium and highest emission scenarios, respectively (Van Vuuren et al. 2011; O'Neill et al. 2016).

Significant warming trends in the projected temperature changes have been found in all three seasons, with the strongest ones over the north catchment occurring in ON particularly during the near term period. The trend for this ON season over the north catchment under the SSP245 (SSP585) scenario projected by the model average is 0.56 °C/decade (0.67 °C/decade), which does not differ much with trend magnitudes projected by the individual models [CESM 0.73 °C/decade (0.48 °C/decade), CMCC 0.79 °C/decade (0.59 °C/decade), MPI 0.30 °C/decade (0.87 °C/decade)]. The projected warming trends are stronger during the long term period than during the near term period particularly under the SSP585 scenario. During the long term period under the SSP585 scenario over the north catchment, the model average projects trends of 1.20 °C/decade, 0.98 °C/decade and 0.85 °C/decade, in ON, DJF and MA, respectively, which are similar to those projected by the individual models [CESM (1.02 °C/decade, 1.09 °C/decade, 0.86 °C/decade), CMCC (0.87 °C/decade, 0.70 °C/decade, 0.54 °C/decade), MPI (1.51 °C/decade, 1.06 °C/decade, 1.00 °C/decade)].

Projected warming trends during the near term and long term periods over Ngamiland are similar to those found over the north catchment, although they are overall larger over the former region than over the latter region. For example, over Ngamiland during the long term period under the SSP585 scenario, the model average projects trends of 1.11 °C/decade, 1.07 °C/decade and 0.90 °C/decade, in ON, DJF and MA, respectively, which are overall larger than those projected over the north catchment (already mentioned). Over both regions, generally the models project stronger trends in temperature changes under the SSP585 scenario than under the SSP245 scenario. The warming trends found here are consistent with those found by other studies over southern Africa (Engelbrecht et al. 2015; Maúre et al. 2018; Almazrroui et al. 2020).

4 Conclusions

This study has examined changes in rainfall and temperature over the Okavango River Basin (ORB) region and its sub-regions (north catchment, Ngamiland) during future periods [2030–2059 (near term period) and 2070–2099 (long term period)] relative to the historical period (1985–2014). CMIP6 model (CESM, CMCC, MPI, and the model average) projections under the SSP245 and SSP585 emission scenarios have been used, focusing on the extended rainy season October–April split into October–November (ON), December-February (DJF) and March–April (MA).

It has been found that historical simulations from the individual models and the model average generally overestimate the observed rainfall and temperature annual cycles during the historical period (1985–2014), as well as the observed interannual variability in the changes of these variables. Future changes in rainfall and temperature have therefore been analysed using bias corrected (method described in Section 2) model projections. All the models show a mixture of reductions and increases in average rainfall during both future periods (near term and long term). For example, for the near term period under the SSP585 (SSP245) scenario over the north catchment, the model average projects an average rainfall change of 0.01 mm/day (-0.02 mm/day) in DJF, in the same season the CESM and MPI project -0.11 mm/day (0.06 mm/day) and 0.14 mm/day (-0.13 mm/day), respectively, and the CMCC projects -0.09 mm/day (-0.07 mm/day) in ON. Future changes in DJF and MA rainfall over Ngamiland are larger than those over the north catchment, whereas in ON, it is the reverse. Over both regions, projected rainfall changes under the SSP245 scenario are not necessarily larger or smaller than those projected under the SSP585 scenario.

The models show some significant decreasing trends in future rainfall over Ngamiland, but none are significant over the north catchment. During the near term period, those significant trends are projected by the CESM (63.90 mm/decade in DJF under SSP245), MPI (-28.20 mm/decade in MA under SSP245) and the model average (-30.60 mm/decade in MA under SSP585). During the long term period, those significant trends occur only in DJF under the SSP585 scenario and are projected by the CESM (-49.50 mm/decade), CMCC (-87.20 mm/decade), MPI (-74.70 mm/decade) and the model average (-85.50 mm/decade).

For temperature, over the north catchment under the SSP585 (SSP245) scenario during the long term period, the model average projects average warming values of 5.36 °C (3.53 °C), 4.37 °C (2.44 °C) and 4.35 °C (2.37 °C), in ON, DJF and MA, respectively, whereas during the near term period, it projects 2.42 °C (1.82 °C), 1.86 °C (1.19 °C), 1.78 °C (1.39 °C). The individual models project average warming values that are similar to those projected by the model average, with those projected by the CESM being generally the largest during both the long term period [6.20 °C (3.54 °C), 5.90 °C (3.25 °C) and 5.37 °C (2.77 °C)] and the near term period [2.71 °C (2.10 °C), 2.51 °C (1.82 °C) and 2.03 °C (1.88 °C)]. Overall, the projected average warming is larger over Ngamiland than over the north catchment. Over both regions, the projected average temperature changes are larger during the long term period than during the near term period. As expected, the average warming projected under the SSP585 scenario is larger than that projected under the SSP245 scenario.

There are significant warming trends in the projected temperature changes in all three seasons. Over the north catchment, particularly during the near term period, the strongest ones occur in ON. These warming trends

under the SSP245 (SSP585) scenario projected by the model average, CESM, CMCC and the MPI are 0.56 °C/decade (0.67 °C/decade), 0.73 °C/decade (0.48 °C/decade), 0.79 °C/decade (0.59 °C/decade) and 0.30 °C/decade (0.87 °C/decade), respectively. Also, during the long term period the warming trends projected by the individual models are similar, with those projected by the model average being 1.20 °C/decade, 0.98 °C/decade and 0.85 °C/decade, in ON, DJF and MA, respectively, under the SSP585 scenario over the north catchment. The results of this study may help with the management of agricultural activities, water resources and the highly biodiverse and sensitive ecosystems in the ORB region.

Data availability No datasets were generated or analysed during the current study.

Declarations

Competing interests The authors declare no competing interests.

References

Almazroui M, Saeed F, Saeed S, Nazrul Islam M, Ismail M, Klutse NAB, Siddiqui MH (2020) Projected change in temperature and precipitation over Africa from CMIP6. ESEV 4:455–475

Andersson L, Gumbricht T, Hughes D, Kniveton D, Ringrose S, Savenije H, Todd M, Wilk J, Wolski P (2003) Water flow dynamics in the Okavango River Basin and Delta: a pre-requisite for the ecosystems of the Delta. Phys Chem Earth 28:1165–1172

Andersson L, Wilk J, Todd MC, Hughes DA, Earle A, Kniveton D, Layberry R, Savenije HH (2006) Impact of climate change and development scenarios on flow patterns in the Okavango River. J Hydrol 331(1–2):43–57

Ayugi B, Ngoma H, Babaousmail H, Karim R, Iyakaremye V, Sian KTLK, Ongoma V (2021) Evaluation and projection of mean surface temperature using CMIP6 models over East Africa. J Afr Earth Sci 181:104226

Barros VR, Field CB (2014) Climate change 2014–Impacts, adaptation and vulnerability: Regional aspects. Cambridge University Press

Blamey RC, Kolusu SR, Mahlalela P, Todd MC, Reason CJC (2018) The role of regional circulation features in regulating El Niño climate impacts over southern Africa: A comparison of the 2015/2016 drought with previous events. Int J Climatol 38(11):4276–4295

Bruyère CL, Done JM, Holland GJ, Fredrick S (2014) Bias corrections of global models for regional climate simulations of high-impact weather. Clim Dyn 43:1847–1856

Conway D, Van Garderen EA, Deryng D, Dorling S, Krueger T, Landman W, Lankford B, Lebek K, Osborn T, Ringler C, Thurlow J (2015) Climate and southern Africa's water–energy–food nexus. Nat Clim Chang 5(9):837–846

Copernicus Climate Change Service (2017) ERA5: Fifth generation of ECMWF atmospheric reanalyses of the global climate. Copernicus Climate Change Service Climate Data Store (CDS) available at https://cds.climate.copernicus.eu Accessed 31 Jan 2024

Danabasoglu G (2019) NCAR CESM2-WACCM model output prepared for CMIP6 ScenarioMIP. Earth System Grid Federation. 10026. https://doi.org/10.22033/ESGF/CMIP6

Engelbrecht F, Adegoke J, Bopape MJ, Naidoo M, Garland R, Thatcher M, McGregor J, Katzfey J, Werner M, Ichoku C, Gatebe C (2015) Projections of rapidly rising surface temperatures over Africa under low mitigation. Environ Res Lett 10(8):085004

Eyring V, Bony S, Meehl GA, Senior CA, Stevens B, Stouffer RJ, Taylor KE (2016) Overview of the Coupled Model Intercomparison Project Phase 6 (CMIP6) experimental design and organization. GMD 9(5):1937–1958

Funk C, Peterson P, Landsfeld M, Pedreros D, Verdin J, Shukla S, Husak G, Rowland J, Harisson L, Hoell A, Michaelson J (2015) The climate hazards infrared precipitation with stations a new environmental record for monitoring extremes. Sci Data 2(1):1–21

Gabaake KP, Lucero-Prisno DE III, Thakadu OT, Phaladze NA (2023) A mixed method analysis of the Botswana schistosomiasis control policy and plans using the policy triangle framework. Glob Health Res Policy 8(1):39

Gidden MJ, Riahi K, Smith SJ, Fujimori S, Luderer G, Kriegler E, Van Vuuren DP, Van Den Berg M, Feng L, Klein D, Calvin K (2019) Global emissions pathways under different socioeconomic scenarios for use in CMIP6: a dataset of harmonized emissions trajectories through the end of the century. GMD 12(4):1443–1475

Guilpart N, Grassini P, Van Wart J, Yang H, Van Ittersum MK, Van Bussel LG, Wolf J, Claessens L, Leenaars JG, Cassman KG (2017) Rooting for food security in Sub-Saharan Africa. Environ Res Lett 12(11). https://doi.org/10.1088/1748-9326/aa9003

Hamed KH, Rao AR (1998) A modified Mann-Kendall trend test for autocorrelated data. J Hydrol 204(1–4):182–196

Hart NC, Washington R, Reason CJC (2018) On the likelihood of tropical-extratropical cloud bands in the south Indian convergence zone during ENSO events. J Clim 31(7):2797–2817

Hersbach H, Bell B, Berrisford P, Hirahara S, Horányi A, Muñoz-Sabater J, Nicolas J, Peubey C, Radu R, Schepers D, Simmons A (2020) The ERA5 global reanalysis. QJR Meteorol Soc 146(730):1999–2049

Holland G, Done J, Bruyere C, Cooper CK, Suzuki A (2010) Model investigations of the effects of climate variability and change on future Gulf of Mexico tropical cyclone activity. In Offshore Technology Conference (OTC-20690), Houston

IPCC (2013) Climate Change 2013: The Physical Science Basis. T.F. Stocker et al., Eds., Cambridge University Press

IPCC (2021) Climate Change 2021: The Physical Science Basis. V. Masson-Delmotte et al., Eds., Cambridge University Press

Jamal K, Li X, Chen Y, Rizwan M, Khan MA, Syed Z, Mahmood P (2023) Bias correction and projection of temperature over the altitude of the Upper Indus Basin under CMIP6 climate scenarios from 1985 to 2100. J Water Clim Chang. https://doi.org/10.2166/wcc.2023.180

Kendall MG (1975) Rank correlation methods. Charles Griffin, London

Kgathi DL, Kniveton D, Ringrose S, Turton AR, Vanderpost CH, Lundqvist J, Seely M (2006) The Okavango; a river supporting its people, environment and economic development. J Hydrol 331(1–2):3–17

Liang-Liang L, Jian L, Ru-Cong Y (2022) Evaluation of CMIP6 High-ResMIP models in simulating precipitation over Central Asia. Adv Clim Chang Res 13(1):1–13

Lim Kam Sian KTC, Wang J, Ayugi BO, Nooni IK, Ongoma V (2021) Multi-decadal variability and future changes in precipitation over Southern Africa. Atmosphere 12(6):742

Lindesay JA (1988) South African rainfall, the Southern Oscillation and a Southern Hemisphere semi-annual cycle. J Climatol 8(1):17–30

Lovato T, Peano D (2020) CMCC CMCC-CM2-SR5 model output prepared for CMIP6 ScenarioMIP ssp585. Earth System Grid Federation 10. https://doi.org/10.22033/ESGF/CMIP6.3889

Mann HB (1945) Nonparametric Tests against Trend. Econometric 13(3):245–259

Maruatona PB, Moses O (2022) Assessment of the onset, cessation, and duration of rainfall season over Botswana. MESE 8(2):1657–1668

Maúre G, Pinto I, Ndebele-Murisa M, Muthige M, Lennard C, Nikulin G, Dosio A, Meque A (2018) The southern African climate under 1.5°C and 2°C of global warming as simulated by CORDEX regional climate models. Environ Res Lett 13(6):065002

Mauritsen T, Bader J, Becker T et al (2019) Developments in the MPI-M earth system model version 1.2 (MPI-ESM1.2) and its response to increasing CO2. J Adv Model Earth Syst 11:998–1038

Mbaiwa JE (2004) The socio–economic benefits and challenges of a community–based safari hunting tourism in the Okavango Delta, Botswana. J Tour Stud 15(2):37

Mbaiwa JE (2015) Ecotourism in Botswana: 30 years later. J Ecotourism 14(2–3):204–222

McCarthy JM, Gumbricht T, McCarthy T, Frost P, Wessels K, Seidel F (2003) Flooding patterns of the Okavango wetland Botswana between 1972 and 2000. Ambio 32(7):453–457

Meque A, Pinto I, Maúre G, Beleza A (2022) Understanding the variability of heatwave characteristics in southern Africa. Weather Clim Extremes. 100498. https://doi.org/10.1016/j.wace.2022.100498

Moseid KO, Schulz M, Storelvmo T, Julsrud IR, Olivie D, Nabat P, Takemura T (2020) Bias in CMIP6 models compared to observed regional dimming and brightening trends (1961–2014). Atmos Chem 20:16023–16040

Moses O (2017) Heat wave characteristics in the context of climate change over the past 50 years in Botswana. BNR 49:13–25

Moses O, Gondwe M (2019) Simulation of changes in the twenty-first century maximum temperatures using the statistical downscaling model at some stations in Botswana. MESE 5:843–855

Moses O, Hambira WL (2018) Effects of climate change on evapotranspiration over the Okavango Delta water resources. Phys Chem Earth, Parts a/b/c 105:98–103

Moses O, Blamey RC, Reason CJC (2022) Relationships between NDVI, river discharge and climate in the Okavango River Basin region. Int J Climatol 42(2):691–713

Moses O, Blamey RC, Reason CJC (2023a) Drought metrics and temperature extremes over the Okavango River basin, southern Africa, and links with the Botswana high. Int J Climatol. https://doi.org/10.1002/joc.8215

Moses O (2023) Climate variability and extremes in the Okavango River Basin, southern Africa. PhD Thesis, University of Cape Town

Moses O, Blamey RC, Reason CJC (2023b) Extreme rainfall events over the Okavango river basin, southern Africa. Weather Clim Extrem 100589. https://doi.org/10.1016/j.wace.2023.100589

Munday C, Washington R (2017) Circulation controls on southern African precipitation in coupled models: The role of the Angola Low. J Geophys Res 122(2):861–877

Munday C, Washington R (2019) Controls on the diversity in climate model projections of early summer drying over southern Africa. J Clim 32:3707–3725

Murray-Hudson M, Wolski P, Ringrose S (2006) Scenarios of the impact of local and upstream changes in climate and water use on hydroecology in the Okavango Delta, Botswana. J Hydrol 331(1–2):73–84

O'Neill BC, Tebaldi C, Van Vuuren DP, Eyring V, Friedlingstein P, Hurtt G, Knutti R, Kriegler E, Lamarque JF, Lowe J, Meehl GA (2016) The scenario model intercomparison project (ScenarioMIP) for CMIP6. GMD 9(9):3461–3482

Pincus R, Batstone CP, Hofmann RJP, Taylor KE, Glecker PJ (2008) Evaluating the present-day simulation of clouds, precipitation, and radiation in climate models. J Geophys Res Atmos 113(D14). https://doi.org/10.1029/2007JD009334

Reason CJC, Jagadheesha D (2005) A model investigation of recent ENSO impacts over southern Africa. Meteorol Atmos Phys 89(1–4):181–205

Reason C, Allan R, Lindesay J, Ansell T (2000) ENSO and climatic signals across the Indian Ocean Basin in the global context: Part I, interannual composite patterns. Int J Climatol 20(11):1285–1327

Reason CJC, Landman W, Tennant W (2006) Seasonal to decadal prediction of southern African climate and its links with variability of the Atlantic Ocean. Bull Am Meteorol Soc 87(7):941–955

Richardson H (2021) A big oil project in Africa threatens fragile Okavango region. Available from: https://e360.yale.edu/features/a-big-oil-project-in-africa-threatens-the-fragile-okavango-region Accessed 10 Feb 2024

Schupfner M, Wieners KH, Wachsmann F, Steger C, Bittner M, Jungclaus J, Früh B, Pankatz K, Giorgetta M, Reick C, Legutke S (2019) CMIP6 CMIP DKRZ MPI-ESM1–2-HR amip-RCM-forcing data. https://doi.org/10.26050/WDCC/RCM_CMIP6_AMIP-HR

Thoithi W, Blamey RC, Reason CJC (2021) Dry spells, wet Days, and their trends across Southern Africa during the summer rainy season. Geophys. Res Lett 48(5):e2020GL091041

Tyson PD (1986) Climatic change and variability in southern Africa. Oxford University Press, USA

UNESCO (2014) Okavango Delta. Available from: http://whc.unesco.org/en/list/1432 Accessed 25 Jan 2024

Van Vuuren DP, Edmonds J, Kainuma M, Riahi K, Thomson A, Hibbard K, Hurtt GC, Kram T, Krey V, Lamarque JF, Masui T (2011) The representative concentration pathways: an overview. Clim Change 109:5–31

Wainwright CM, Black E, Allan RP (2021) Future changes in wet and dry season characteristics in CMIP5 and CMIP6 simulations. J Hydrometeorol 22(9):2339–2357

Wolski P, Murray-Hudson M (2008) "Alternative futures" of the Okavango Delta simulated by a suite of global climate and hydro-ecological models. Water SA 34(5):605–610

Xu Z, Han Y, Tam CY, Yang ZL, Fu C (2021) Bias-corrected CMIP6 global dataset for dynamical downscaling of the historical and future climate (1979–2100). Sci Data 8(1):293

Yue S, Wang CY (2002) Applicability of prewhitening to eliminate the influence of serial correlation on the Mann-Kendall test. Water Resour Res 38(6):4–1